



University of
Massachusetts
Amherst

SCREENING FOR OXIDATIVE STRESS ELICITED BY ENGINEERED NANOMATERIALS: EVALUATION OF ACELLULAR DCFH ASSAY

Item Type	Article
Authors	Pal, Anoop K.;Bello, Dhimiter;Budhlall, Bridgette;Rogers, Eugene
Download date	2026-03-15 14:18:20
Link to Item	https://hdl.handle.net/20.500.14394/20325

SCREENING FOR OXIDATIVE STRESS ELICITED BY ENGINEERED NANOMATERIALS: EVALUATION OF ACELLULAR DCFH ASSAY

Anoop K. Pal, Dhimiter Bello, Bridgette Budhlall, Eugene Rogers □ University of Massachusetts Lowell

Donald K. Milton □ University of Maryland College Park

□ The DCFH assay is commonly used for measuring free radicals generated by engineered nanomaterials (ENM), a well-established mechanism of ENM toxicity. Concerns exist over susceptibility of the DCFH assay to: assay conditions, adsorption of DCFH onto ENM, fluorescence quenching and light scattering. These effects vary in magnitude depending on ENM physicochemical properties and concentration. A rigorous evaluation of this method is still lacking. The objective was to evaluate performance of the DCFH assay for measuring ENM-induced free radicals. A series of diverse and well-characterized ENM were tested in the acellular DCFH assay. We investigated the effect of sonication conditions, dispersion media, ENM concentration, and the use of horseradish peroxidase (HRP) on the DCFH results. The acellular DCFH assay suffers from high background signals resulting from dye auto-oxidation and lacks sensitivity and robustness. DCFH oxidation is further enhanced by HRP. The number of positive ENM in the assay and their relative ranking changed as a function of experimental conditions. An inverse dose relationship was observed for several Carbon-based ENM. Overall, these findings indicate the importance of having standardized assays for evaluating ENM toxicity and highlights limitations of the DCFH assay for measuring ENM-induced free radicals.

Keywords: DCFH, engineered nanomaterials, oxidative stress, ROS, toxicity screening

INTRODUCTION

Extensive scientific research and investments have been made in the field of nanotechnology, leading to high rate, high volume manufacturing of a variety of engineered nanomaterials (ENM). It has been estimated that the production of ENM would increase approximately 25 fold from a few thousand tons produced today to 58,000 tons by 2020 (Maynard 2006; Nastassja et al. 2008) with possible applications in a range of diverse fields, from development of advanced materials, novel devices in the fields of medicine, biotechnology, energy, environmental remediation to their use in consumer products (Zhang 2003; Salata 2004; Raimondi et al. 2005). In response to this reality, a broad consensus is being built to conduct adequate environmental, health and safety evaluations of these novel ENM at an early stage of materials/product develop-

Address correspondence to Dhimiter Bello, Sc.D., M.Sc., Asst. Professor, Department of Work Environment, School of Health and Environment, University of Massachusetts Lowell, One University Ave., Lowell, MA 01854, USA; Fax: 978 452 5711; Phone: +1 978 934 3343; Email: dhimiter_bello@uml.edu

ment. Major efforts are underway on developing reliable and predictive nanotoxicity screening approaches based on proven toxicological pathways (Meng *et al.* 2009; Donaldson *et al.* 2010). Given the variability in ENM physicochemical properties (e.g. surface area, surface charge, morphology, and surface chemistry) and the large number of resulting combinations, the challenge of timely evaluation of their toxicity can only be met with high throughput, low cost, screening assays (Ayres *et al.* 2008; Bello *et al.* 2009; Lu *et al.* 2009; Meng *et al.* 2009; Xia *et al.* 2009). Although how this will be accomplished is still unresolved, it is likely that a platform of standardized tests, spanning various possible toxicological pathways, may be needed in order to predict the overall toxicity potential of ENM.

Oxidative stress (OS) has been recognized in vivo and in vitro systems as one such major pathway and is being explored for ENM toxicity screening purposes (Nel *et al.* 2006; Xia *et al.* 2006; Borm *et al.* 2007; Ayres *et al.* 2008; Rogers *et al.* 2008; Bello *et al.* 2009; Lu *et al.* 2009; Meng *et al.* 2009). OS has been linked to pathogenesis of several diseases, including neurodegenerative diseases (Calabrese *et al.* 2006), atherosclerosis (Hsiai and Berliner 2007; Bonomini *et al.* 2008), cancer (Lau *et al.* 2008; Mates *et al.* 2008; Nishikawa 2008), diabetes mellitus (Bekyarova *et al.* 2007; Forbes *et al.* 2008), hypertension, (Paravicini and Touyz 2008), and other inflammatory conditions. OS has also been implicated as an important pathway in metal toxicity (Valko *et al.* 2005; Valko *et al.* 2006), and several commercially important classes of ENM are either metals or metal oxides themselves or contain significant amounts of metal catalysts (such as CNTs).

Several assays relying on the detection of free radicals generated in the test system have been employed for OS screening. The DCFH, ESR and DTT are commonly used assays for quantitating ROS elicited by ENM (Sauvain *et al.* 2008). The DCFH assay has been around since 1940s and has been used for measuring several endpoints, such as determining monoamine oxidase activity (Degli-Esposti *et al.* 2001), serum uric acid and glucose concentrations (Kato *et al.* 1979) and identify spermine in seminal stains (Suzuki *et al.* 1980). An excellent summary of the DCFH assay history and applications has been published recently (Chen *et al.* 2010). Modified variants of the DCFH assay have also been used for nanotoxicity studies in a cell-free (acellular) environment and on a variety of cell lines (Wilson *et al.* 2002; Arbab *et al.* 2003; Manna *et al.* 2005; Foucaud *et al.* 2007; Doak *et al.* 2009; Lu *et al.* 2009; Xia *et al.* 2009). Because DCFH detects a wide range of ROS (RO_2 , RO , OH , HOCl and ONOO but not O_2^- and H_2O_2), it is simple and inexpensive to set up and offers 96-well plate automated capabilities, it has gained popularity for measuring ROS induced by ENM (Doak *et al.* 2009).

The DCFH assay, like most of the other conventional colorimetric (dye-based) assays that have been used for ENM toxicity evaluations (such as 3-(4,5-dimethylthiazol-2-yl)-2,5-diphenyltetrazolium bromide (MTT), 2-(4-iodophenyl)-3-(4-nitrophenyl)-5-(2,4-disulfophenyl)-2H-tetrazolium (WST-1), Neutral Red and Alamar Blue™) were originally standardized and optimized for chemical compounds and were adopted with little modifications and method evaluation for ENM. Because of the fundamental differences in the physicochemical properties and behavior between ENM and organic molecules, the assumption that ENM can be tested similarly to other chemicals needs to be proven and anecdotal evidence is building up against the DCFH assay (Doak *et al.* 2009). Interaction of these indicator dyes with carbon-based ENM may provide erroneous results (Hurt *et al.* 2006; Monteiro-Riviere and Inman 2006; Wörle-Knirsch *et al.* 2006; Belyanskaya *et al.* 2007; Casey *et al.* 2007; Monteiro-Riviere *et al.* 2009), which raises concerns over applicability of the organic dye-based assays for ENM toxicity evaluations (Casey *et al.* 2007). Unreliable assays may generate confusion caused by conflicting and irreproducible data, and questioning of the utility of OS as a marker for nanotoxicity evaluations.

The DCFH assay provides a measure of several ROS and RNS species and is useful when such a global metric is desirable, such as for toxicity screening. Its utility is more constrained for mechanistic studies; such as if one needs to measure specific ROS/RNS radicals and identify their source/origin (Tarpey and Fridovich 2001; Doak *et al.* 2009). The DCFH, however, suffers from several well-known problems (Chen *et al.* 2010). One major problem intrinsic to the DCFH is its unstable nature. The DCFH dye is slowly oxidized to the fluorescent DCF species in air and is also prone to photo-oxidation by the laser light utilized for fluorescence excitation. Thus, DCFH detection can generate false-positive results (Sarvazyan 1996; Wang and Joseph 1999) and background values increase with time. A summary of potential sources of error in the DCFH assay is provided in Table 1.

In this study, we look systematically at several factors (summarized in Table 1) that may compromise the DCFH performance for ENM ROS measurement, including: the type of nanomaterial, ENM concentration, sonication conditions, dispersion media, and the effect of horseradish peroxidase (HRP) on the DCFH stability and ROS generation. HRP has been added to ENM to mimic the cellular conditions of ROS production (Foucaud *et al.* 2007; Jiang *et al.* 2008; Rothen-Rutishauser *et al.* 2010). This paper provides multiple lines of evidence that the DCFH assay is susceptible to several experimental parameters and that in its current format the assay is not well suited for ENM ROS measurements.

TABLE 1. Potential errors can be introduced at various steps of the DCFH assay when it is used for the measurement of reactive oxygen species generated by engineered nanomaterials (ENMs). We grouped them into three broad steps: (i) Preparation of ENM dispersions; (ii) Interaction of ENM with the assay measurement principle; and (iii) System interdependence on nanomaterial properties.

Step	Investigated	Potential effects
Dispersion:^a		
Medium	1% BSA/0.9% NaCl	<ul style="list-style-type: none"> • Dispersion efficiency (size distribution and homogeneity); • Dispersion stability; • Interaction of ENMs with proteins and other components of the dispersion medium affecting surface activity of ENMs;
	Surfactant, Triton-X 100	
Energy	High energy cup sonication ~ 125W	<ul style="list-style-type: none"> • Structural defects and size fracturing of ENMs by sonication; • Generation of free radicals during sonication;
	Ultrasonic probe sonication ~ 225W	
Assay Conditions:		
Measurement Time / Reaction kinetics	0-120 min	<ul style="list-style-type: none"> • Reaction kinetics may vary depending on ENM type, thus measurements have to be made near reaction completion; • Re-agglomeration of ENMs in the well plate during measurements may lead to settling of agglomerates and changes in effective dose;
	0.1, 0.3, 0.5 mg/mL	
ENM concentration	DCFH oxidation by HRP	<ul style="list-style-type: none"> • Potential adsorption/removal of DCFH by ENMs; • Interaction of ENMs with optical measurements (e.g. light scattering and absorption, or fluorescence quenching); • Stronger effects are likely to occur at higher ENMs concentrations; • HRP-catalyzed oxidation of the DCFH dye; Effects may be modulated by the dispersion medium;
	Assaying of ENM in the absence of HRP	
ENMs type:	C-based ENM Metals/Metal Oxides	<ul style="list-style-type: none"> • Different sizes, specific surface areas and surface activities may lead to different levels of absorption of DCFH, HRP inactivation, as well as interaction with the light beam; • Additional effects may be impacted by impurities in the ENM, e.g. transition metals selectively deactivating HRP or organic impurities absorbing in the same region as DCFH itself.
	Series of different sizes and impurities	

^a Although important, dispersion is a generic issue for ENM and not specific to DCFH.

MATERIALS AND METHODS

Chemicals and reagents

The 2'-7'-DiChlorofluorescein Diacetate (DCFH-DA) dye, NaOH, Phosphate Buffer Saline (PBS), H₂O₂, Bovine serum albumin (BSA), Horseradish peroxidase (HRP) and Triton X-100 were obtained from Sigma–Aldrich (Sigma, St. Louis, MO). Methanol was purchased from Burdick and Jackson (Muskegon, MI, USA). All chemicals were of analytical grade and were used as received.

Nanomaterials

For the purpose of investigating the DCFH response to different ENM types, a well characterized set of 19 materials of commercial importance and with a broad range of physicochemical properties, were selected. The ENM used in the study, are summarized in Table 2. The materials together with their sources and specifications have been described previously by us (Bello *et al.* 2009) and included a series of carbon blacks, a series of fullerenes, a series of titanium dioxides (nano- and micron-sized anatase and rutile), a series of single and multi-wall carbon nanotubes (CNTs) of variable length and purity, H₂O₂-oxidized single wall carbon nanohorns (SWCNHs-ox), nano alumina, nano silver, and micron-sized crystalline silica. For simplicity, we will refer to the whole set of materials under investigation as ENM, although some are microscopic.

Physicochemical characterization

The initial set of 19 ENM has been previously reported (Bello *et al.* 2009) and includes: Specific Surface Area (SSA), total and water-soluble transition metals, organic and elemental carbon (OC/EC), surface charge in PBS saline and crystallinity. Procedures for each characterization technique are detailed in Bello *et al.* 2009.

Dispersion of Nanomaterials

Efficient dispersion of ENM at or near the primary particle size dimensions remains a serious challenge and different ENM classes may require different protocols for best dispersion. Because sonication itself may introduce artifacts (such as the generation of free radicals, modification of the dispersion medium and the ENM themselves), it is important that all ENM to be tested for comparative evaluations get dispersed under the same protocol. Initial work investigated dispersion efficiency of the whole ENM set in two dispersion media, one analogous to a biologically relevant medium of 1% wt. BSA/0.9 wt % NaCl_{aq} (Bihari *et al.* 2008) and the other in the chemical surfactant 0.07% wt. Triton X-100 (Hilding *et al.* 2003; Moore *et al.* 2003; Saran *et al.* 2004). For this study three independent stock solutions of 0.8-1.0 mg/mL were prepared for each ENM in each medium on different days and each stock was assessed at least three times in triplicates. That is a minimum of nine measurements were available for each ENM/condition combination. Sonication to prepare dispersions was performed using a 400 W Branson 450D sonifier with a 550 dismembrator. In our work, three distinct dispersion conditions were investigated: (i) ENM dispersed in 1% BSA / 0.9 % NaCl_(aq) for 12 min with cup sonication (~90W), (ii) ENM dispersed in 1%_(aq) BSA / 0.9% NaCl_(aq) for 10 min with 30 sec cycle at 30% amplitude probe sonication (~200W); and (iii) ENM dispersed in 0.07% Triton X-100 for 10 min with

30 sec cycle at 30% amplitude probe sonication (~200W). The scintillation vials containing ENM solutions were kept in ice and capped during the whole cup sonication process, whereas for probe sonication vials were kept in ice uncapped. Because the primary purpose of this set of experiments was to investigate the magnitude of susceptibility of the assay to sonication/dispersion conditions (which continues to be a non standardized process) and not a strict comparison of dispersion protocols, some variations in the sonication cycle settings were deemed acceptable.

Dispersion efficiency of ENM in each dispersion condition was determined in triplicate by taking intensity weighted particle size measurements using a dynamic light scattering (DLS) Malvern Zetasizer Nano-ZS instrument. The Zetasizer is equipped with a monochromatic coherent 4mW Helium Neon laser ($\lambda = 633$ nm) with a 173° scattering angle and with a non-invasive back-scatter (NIBS) technology for increasing particle size sensitivity. The measurements are reported as the z-average hydrodynamic diameter ($d_{h,z\text{ ave}}$) and the particle size polydispersity index (PDI), which is a measure of the broadness of the particle size distribution. The PDI scale ranges from 0 to 1, with 0 being monodisperse and 1 being polydisperse (Bihari *et al.* 2008). The measurements were performed within 5 minutes after sonication, and before and after each measurement, the electrophoretic cell was washed with distilled and deionized water to prevent cross contamination. The temperature of the laboratory was kept at 22 ± 2.5 °C during all experiments. In brief, during DLS measurements the particles are subjected to Brownian motion. This is compensated by normalization of the electric field autocorrelation function, of which the cumulative analysis is used to obtain the z-average hydrodynamic diameter ($d_{h,z\text{ ave}}$). The autocorrelation function is calculated by the Stokes–Einstein equation with the diffusion coefficient determined from the decay time of autocorrelation function. In addition there is certain probability that the light scattered by larger particles will swamp the light scattered by smaller particles since the light intensity of a scattered particle is proportional to the diameter in the sixth power. That means that larger particles are overestimated in the dispersions. For this reason the change of $d_{h,z\text{ ave}}$ with ultrasonic treatment time shows only a trend in the change of particle size (Krause, *et. al.*, 2010).

The Acellular DCFH assay

We used the modified DCFH method as described in previous publications (Foucaud *et al.* 2007; Bihari *et al.* 2008) for dispersion, as well as the ROS measurements. Briefly, in the DCFH assay 15 μ l of 1 mM DCFH-DA dye was chemically hydrolyzed to DCFH with 50 μ l of 0.01N NaOH in each well of 96-well ELISA plate. The reaction plate was placed in dark at room temperature for 30 minutes. Following hydrolysis of DCFH-DA, 170 μ l of 0.1M PBS was added in the 96-well plates. Then, ENM solution was

spiked in triplicates to give a final concentration of 0.1, 0.3, or 0.5 mg/mL in wells. Alongside, a blank (no ENM added) and a positive control (H_2O_2) were used in the assay, both in triplicates. In the wells containing H_2O_2 , HRP (0.01U) was added. No HRP was added to wells containing ENM. After addition of HRP to the H_2O_2 wells (positive controls and calibration standards), the plate was placed on ice and assayed rapidly. The fluorescence generated by the DCFH oxidation was measured continuously for 120 min at 485 nm excitation and 530 nm emission both with a slit-width of 10 nm under constant agitation condition and constant temperature of 37 °C. Readings were taken at time zero and every 10 min intervals for 120 min. The data reported is for 90 min reaction time-frame, a decision that was based on initial reaction kinetics evaluations. Fluorescence values obtained for ENM were converted to H_2O_2 equivalents against a calibration curve of H_2O_2 in the range of 0-1000 μM H_2O_2 with an $r^2 = 0.999$. This conversion is not necessary for the purpose of the paper. However, conversion of arbitrary fluorescence units to a biologically meaningful ROS value is desirable and one approach used for ENM is conversion in H_2O_2 -equivalents (Foucaud et al. 2007; Jiang et al. 2008; Lu et al. 2009). Because H_2O_2 cannot oxidize DCFH independently, the enzyme HRP is added to catalyze generation of OH radicals. Therefore, HRP was added only when H_2O_2 was used as positive control and for the standards.

Effect of HRP on DCFH oxidation

Considerable discrepancies and confusion exists in the literature with regards to the practice of adding HRP to ENM, its concentration, and the sequence of events with regards to its use (when exactly is HRP added in reaction mixture). We have not found convincing scientific rationale for addition of HRP to ENM. Since oxidation of DCFH by HRP has been reported over a decade ago (Rota *et al.* 1999a; Rota *et al.* 1999b), this raises concerns over its use in the DCFH assay for ROS measurements of ENM. It has also been reported that the HRP catalytic activity may be modulated (deactivated or enhanced) by several transition metals (e.g. Mn, Co, and Ni), which are common in carbon nanotubes and other metal oxides (Mahmoudi *et al.* 2003). Therefore, a systematic investigation of the effect of HRP on DCFH was undertaken. HRP effect (0.01U final concentration) was investigated on blanks (no ENM added) under different conditions, including the sequence of adding HRP and sonication. Several experiments were grouped into three broad conditions: effect of HRP on blanks with and without sonication and effect of event sequence of HRP addition. As an illustration, we investigated the DCFH fluorescence of blanks when reagents were added in the following order: (i) DCFH, NaOH, PBS; (ii) DCFH, NaOH, PBS plus HRP; and (iii) DCFH, NaOH, PBS, HRP + dispersant (BSA or Triton X-100) plus sonication.

Statistical Analysis

Experimental data was investigated for normality of distributions and differences in means between test systems were analyzed via two-sided t-test, analysis of variance ANOVA, correlation and regression using SPSS v18 (SPSS Inc., Chicago, IL, USA). The error bars in DCFH response figures represent the 95% Confidence interval (CI) of at least three independent ENM dispersions tested in triplicate.

RESULTS

Effect of HRP on DCFH oxidation

Results of the investigation of HRP on DCFH response are summarized in Figure 1. For blanks without HRP (experiment 1, 4 and 7) the DCFH response is comparable at $\sim 100 \mu\text{M H}_2\text{O}_2 \text{ Eq.}$ and notably lower than for all other experiments that involved HRP. Addition of HRP to blanks increased fluorescence response by $\sim 4\text{-}5$ times regardless of sonication (experiments 2 and 3 vs. 5 and 6 relative to 1, 4, and 7). The worst situation was observed for experiment 8 (addition of HRP in Triton X-100 dispersion media followed by sonication). The sequence of events

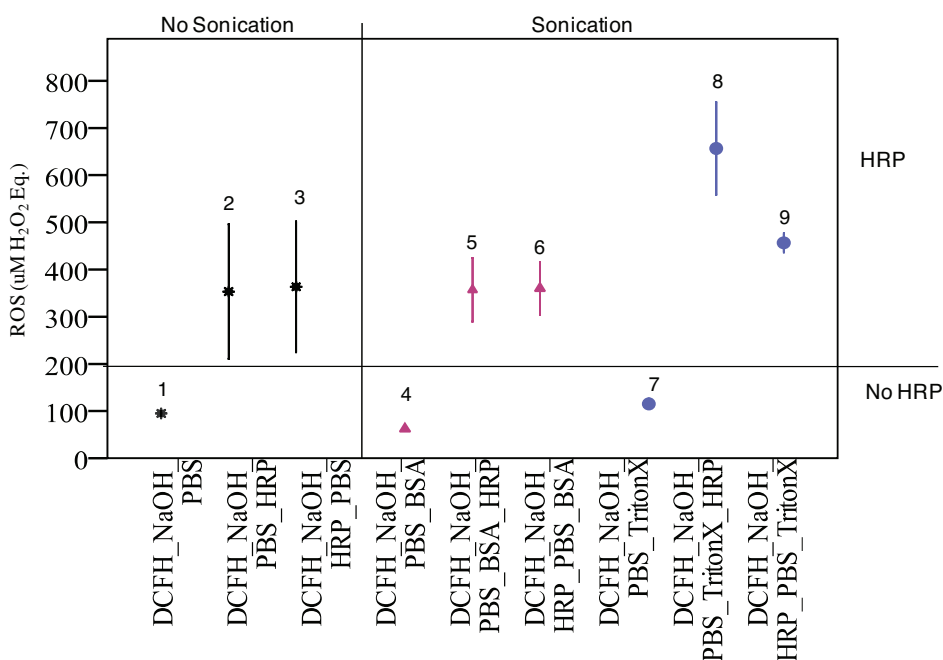


FIGURE 1. Effect 0.01U of HRP on DCFH oxidation of blanks (no nanomaterials involved) under different conditions (sequence of events and dispersion conditions). The label on the X-axis reflects actual sequence of events. HRP is undoubtedly involved in DCFH oxidation and the magnitude of the effect spans approximately an order of magnitude compared to blanks without HRP, depending on the experimental conditions.

apparently may be important in some circumstances (e.g. experiment 8 vs. 9) but not others (2 and 3 vs. 5 and 6). Dispersion medium also plays a significant modifying role on the effect of HRP on DCFH as can be clearly seen in the differences between 1%BSA/0.9%NaCl_{aq} medium (experiments 5 and 6) and Triton X-100 (experiments 8 and 9). HRP is undoubtedly involved in DCFH oxidation and the magnitude of the effect spans approximately an order of magnitude compared to blanks without HRP, depending on the experimental conditions. Based on these results we could not justify the addition of HRP onto ENM for ROS measurements.

Dispersion Efficiency

Dispersion efficiency results for the complete set of 19 ENM in all three conditions are presented in Table 2. The z-average hydrodynamic diameter ($d_{h,z\text{ ave}}$) and polydispersity index (PDI) of the dispersions were determined using DLS and were used as a measure of dispersion efficiency. The $d_{h,z\text{ ave}}$ of all ENM (except TiO₂-Rutile in Triton X-100) in each of the three dispersion conditions tested were consistently higher than the primary particle size of ENM. Thus, the particles aggregated and agglomerated considerably in the dispersion conditions. Better dispersions (lower $d_{h,z\text{ ave}}$ and PDI values) were obtained for the majority of ENM in 1% BSA / 0.9 % NaCl_(aq) as the sonication energy increased (cup sonication vs. probe sonication). Using 0.07 % Triton X-100 and high energy probe sonication even better dispersions for ENM were obtained, except for SWCNT_L, TiO₂-mR and Al₂O₃. In general, higher dispersion stability was observed for ENM dispersed in 0.07 % Triton X-100 than for ENM dispersed in 1% BSA / 0.9 % NaCl_(aq) irrespective of energy used. (DLS measurements were conducted over 90 min for a few ENM to confirm these interpretations, data not shown).

We obtained $d_{h,z\text{ ave}}$ and PDI values for the entire carbon black series tested and the distribution of particles was such that 90% or more particles was found in the primary peak. The $d_{h,z\text{ ave}}$ increased from N110 to N990, reflecting the same trend as their primary particle size. For example, N990 (primary size > 200 nm) had consistently larger $d_{h,z\text{ ave}}$ values than N550 (44 nm). For the fullerene series, values obtained showed variability both in $d_{h,z\text{ ave}}$ and PDI due to a high rate of particle agglomeration (due to its strong hydrophobic nature) in solution under all tested conditions. Irrespective of dispersion conditions, high PDI was obtained with < 70% particle found in the primary peak of the particle size distribution (PSD) for Fullerene_purified.

Comparable values were obtained for two SWCNT in all dispersion conditions. For SWCNT_L, however, the $d_{h,z\text{ ave}}$ value in 0.07 % Triton X-100 was half of that obtained in 1 % BSA / 0.9% NaCl_(aq) without any considerable change in PDI but with fluctuations in number of particles in

primary peak. In the series of MWCNT tested, values for $d_{h,z\text{ ave}}$ and PDI consistently decreased for all three MWCNT tested, with a major decrease in both $d_{h,z\text{ ave}}$ and PDI for MWCNT_L ($d_{h,z\text{ ave}}$ from 471.6 nm to 124.2 nm and PDI from 0.48 to 0.19). SWCNHs-ox had nearly identical values in all

TABLE 2. Dispersion efficiency of different ENMs for three different sonication conditions. These materials have been fully characterized and were previously reported (Bello et al. 2009). Legend: SSA, Specific Surface Area; Z-Ave – Average particle size as measured by DLS; PDI – Polydispersity index. ^a Represents the primary peak (90% or more of the overall distribution); ^b This peak represented primary peak (>75% of the overall distribution). ^c Represents the primary peak (< 75% of the overall distribution).

Label	Material	Primary particle size	SSA m ² g ⁻¹	Dispersion Conditions and Results ^a					
				1 wt.% BSA + 0.9 wt.% NaCl			0.07 wt.% Triton-X-100		
				Cup Sonication $d_{h,z\text{ ave}}$ (nm)	PDI	$d_{h,z\text{ ave}}$ (nm)	Probe Sonication $d_{h,z\text{ ave}}$ (nm)	PDI	PDI
N110	Carbon black N110	15 nm	110.6	256.30	0.23	184.70	0.16	177.15	0.18
N550	Carbon black N550	44 nm	39.23	338.20	0.23	272.40	0.21	292.45	0.27
N990	Carbon black N990	>200 nm	7.74	542.37	0.30	569.10	0.33	487.40	0.11
F_soot	Fullerene soot (>7% wt fullerenes)	>20 nm	194.3	297.93	0.15	198.50	0.16	190.75	0.14
F_refined	Fullerene (refined, 75% C ₆₀ , 22% C ₇₀ , 3% >C ₇₀)	>20 nm	1.27	393.87	0.57	388.50	0.35	358.55	0.37
F_purified	Fullerene, purified (>99% C ₆₀)	>20 nm	0.2	112.27 ^c	0.72	372.60	0.37	312.30	0.38
SWCNT_S	Short Single Wall CNTs; >60% wt	OD = 1-2 nm; L = 0.5-2 μm	342.9	428.67 ^c	0.22	405.70 ^b	0.21	490.20	0.23
SWCNT_L	Long Single Wall CNTs; >90% wt	OD = 1-2 nm; L = 5-30 μm	510.5	1349.67 ^b	0.33	1084.00	0.30	581.20 ^c	0.25
MWCNT_S	Short Multi-Wall CNTs; >95% wt	OD = 10-20 nm; L = 0.5-2 μm	229.1	273.63	0.23	273.70	0.20	233.05	0.20
MWCNT_L	Long Multi-Wall CNTs; >95% wt	OD = 10-30 nm; L = 10-30 μm	156.1	471.60	0.48	191.00	0.21	124.20 ^b	0.19
MWCNT_I	Industrial Grade Multi-Wall CNTs; >90% wt	OD = 10-30 nm; L = 10-30 μm	99.7	371.50	0.47	317.30	0.46	307.05	0.45
SWCNHs-ox	Single Wall Carbon Nanohorns, H ₂ O ₂ oxidized	OD = 1-2 nm; L = 10-30 μm	1154	258.40	0.41	258.70	0.43	221.35	0.54
TiO ₂ _nA	Nano TiO ₂ (Anatase)	10 nm	274.2	224.83	0.35	194.80	0.32	148.50	0.43
TiO ₂ _nR	Nano TiO ₂ (Rutile)	10 nm thick, 40 nm laterally	189.9	312.70	0.30	262.50	0.28	259.05	0.36
TiO ₂ _mA	Micro TiO ₂ (Anatase)	1-5 μm	9.8	238.13	0.35	175.40	0.32	226.90	0.41
TiO ₂ _mR	Micro TiO ₂ (Rutile)	1-5 μm	2.5	712.47	0.73	399.30	0.47	1292.00	0.78
nAg	Nano silver	~60 nm	8.4	324.70	0.45	207.40 ^c	0.16	177.50 ^b	0.17
Silica	Crystalline Silica (Min-U-Sil 5)	>0.1-5 μm	5.1	320.60	0.24	227.10 ^c	0.10	219.30	0.25
nAl ₂ O ₃	Nano alumina	45 nm	28.3	189.83	0.57	190.60	0.64	411.95	0.56

three conditions, although there was a small shift in size and PDI in 0.07 % Triton X-100 condition than 1 % BSA / 0.9 % NaCl_(aq) conditions.

For the metal oxides series comprising titania, nAg, silica, the $d_{h,z,ave}$ decreased for TiO₂-nA, TiO₂-nR, nAg and silica as shown in Table 2 (going from dispersion in 1 % BSA / 0.9 % NaCl_(aq) with cup sonication to dispersion in 0.07 % Triton X-100 with probe sonication). There was no trend in PDI for the same set of ENM. For TiO₂-mA, TiO₂-mR and alumina both the $d_{h,z,ave}$ and PDI show considerable variations depending on the energy and surfactant used for dispersion. As indicated by $d_{h,z,ave}$ and PDI values, Triton X-100 with probe sonication gave overall better dispersion stability than the other two dispersion conditions, with the carbon based nanomaterials being better dispersed than the metal oxides.

ROS generation in the DCFH assay

ROS values for all ENM under different dispersion conditions (reported as $\mu\text{M H}_2\text{O}_2$ equivalents) are presented in Figures 2, 3 and 4. All values are for 0.3 mg/mL of ENM. Data for the other two concentrations (0.1 and 0.5 mg/mL) are presented later. In each figure, the dotted red line indicates the ROS value of the blank (no ENM added) and error bars indicate 95% confidence intervals (95% CI). ENM for which the lower fifth percentile of the distribution was above the red line was considered as a positive result (i.e. the ENM generates ROS, which is statistically significantly greater than the blank value, $p < 0.05$, t-test) on the assay whereas those for which the upper 95th percentile was below the blank were taken to be negative on the assay (i.e. the ENM did not generate ROS values that were higher than the blank; $p > 0.05$, one sided t-test). When the 95% CI of ROS included the red line the test was considered inconclusive, meaning that for a single DCFH measurement (as is commonly done in reality) the ROS value could potentially be positive, although statistically the ENM ROS value was not significantly different than the blank ($p > 0.05$, t-test).

The number of ENM in the positive, negative and inconclusive category varied with the assay conditions. For ENM dispersed in 1% BSA/0.9% NaCl_(aq) using cup sonication (Figure 2) there were 4 positive ENM (SWCNT_S, SWCNT_L, MWCNT_S and SWCNH-ox), 13 negatives (the majority of ENM) and 2 inconclusive (MWCNT_L, nAg). For ENM dispersed in 1% BSA/0.9% NaCl_(aq) using probe sonication (Figure 3) there were 3 positives (SWCNT_S, SWCNT_L and nAg), 12 negatives and 4 inconclusive (MWCNT_L, MWCNT_S, nano Al₂O₃). Interestingly, SWCNH-ox, the ENM with the highest response in cup sonication yielded a negative result and the CI interval was narrower. Additionally, nano Ag switched from inconclusive to positive and MWCNT_S switched from positive to inconclusive. For ENM dispersed in Triton X-100 (Figure 4) there were 5 positives (SWCNT_S, SWCNT_L, MWCNT_S, MWCNT_L

Evaluation of the DCFH assay for ROS measurement

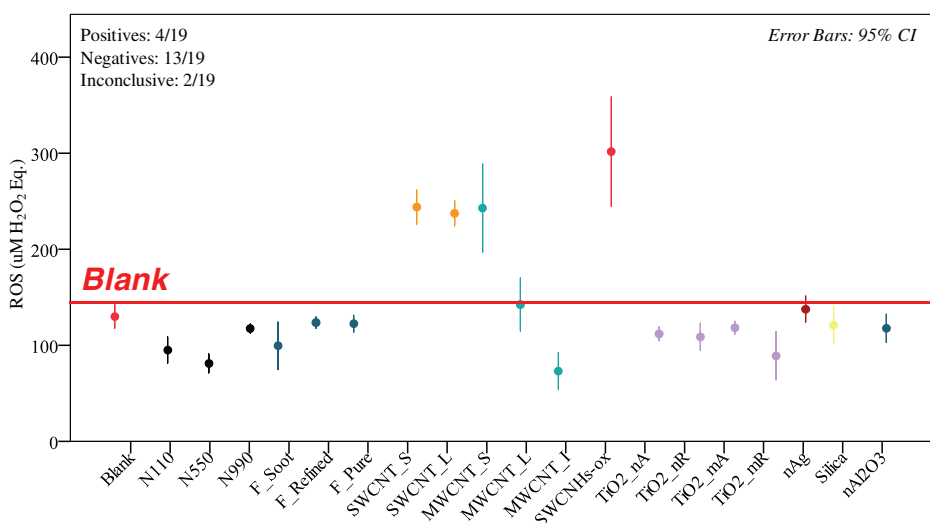


FIGURE 2. DCFH ROS generation of 19 ENMs in 1wt.%BSA/0.9wt. % NaCl_{aq} dispersed by cup sonication. Only 4 of the 19 ENMs were positive (95% confidence interval above blank value denoted with the red line), 13 were negative and two were inconclusive (MWCNT_L, nano Ag). The positive samples included three CNTs and the SWCNHs-ox. Each value represents 3 or more independent sonications, each in triplicates (n≥9).

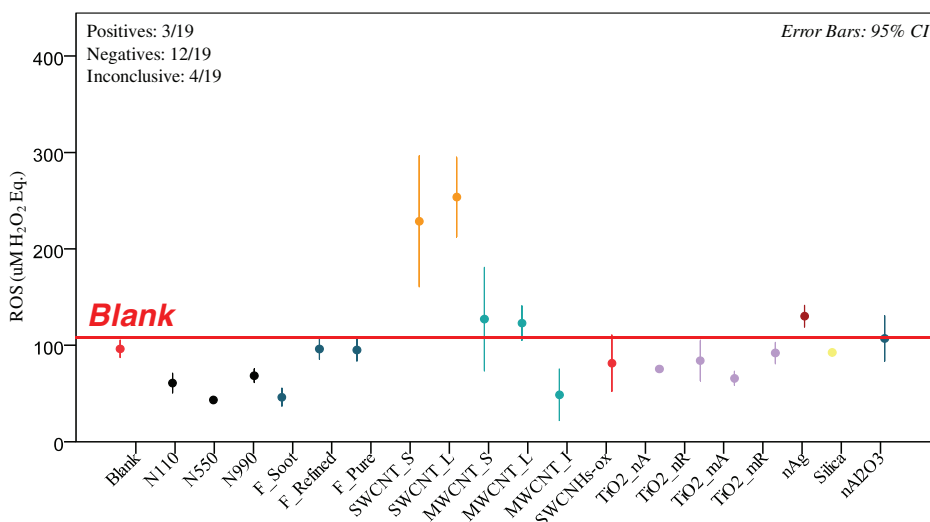


FIGURE 3. DCFH ROS generation of 19 ENMs in 1wt.%BSA/0.9wt.% NaCl dispersed by probe sonication. Only 3 of the 19 ENMs were positive (95% confidence interval above blank value denoted with the red line), 12 were negative and four were inconclusive (MWCNT_L, MWCNT_S, nano Al₂O₃). The positive samples included SWCNT_S, SWCNT_L and nAg. Note also that SWCNHs-ox dropped from the strongest signal in cup sonication (Figure 2) to negative. Each value represents 3 or more independent sonications, each in triplicates (n≥9).

and SWCNHs-ox), 12 negatives and 2 inconclusive (MWCNT_I and nano Ag). Interestingly, SWCNHs-ox gave the highest ROS value again. The CI

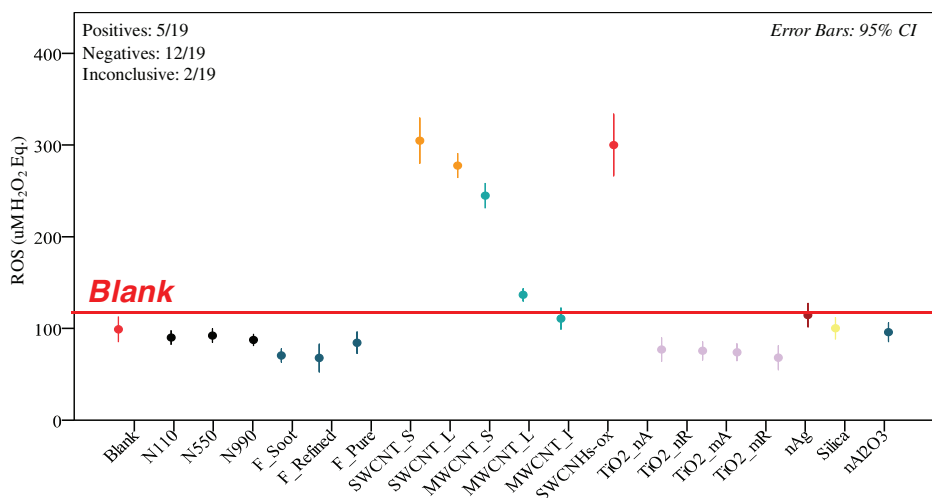


FIGURE 4. DCFH ROS generation of 19 ENMs in 0.7wt.% Triton-X 100 dispersed by probe sonication. Only 5 of the 19 ENMs were positive (95% confidence interval above blank value denoted with the red line), 12 were negative and 2 were inconclusive (MWCNT_I and nano Ag). The positive samples included four CNTs (SWCNT_S, SWCNT_L, MWCNT_S, MWCNT_L) and SWCNHs-ox. Each value represents 3 or more independent sonications, each in triplicates ($n \geq 9$).

intervals were generally narrower for this condition, likely reflective of better and more reproducible dispersion.

The majority of ENM were consistently negative on the DCFH assay, and this included the series of carbon blacks, fullerenes, titania, crystalline silica, and nano alumina (two out of three tests). Important also is the common observation that the majority of the negative ENM gave results that were consistently lower (up to 2x) than the blank value.

Dose Response of ENM

The dose-response for each ENM was studied at three concentrations: 0.1, 0.3 and 0.5 mg/mL. Here we report results for probe sonication in Triton X-100, the condition with overall better dispersion efficiency and stability, and the data are shown in Figure 5. The first general observation is the lack of a proportional DCFH response with increased ENM dose. The highest ENM dose of 0.5 mg/mL gave consistently a much lower response than the lowest dose (0.1 mg/mL). The 0.3 mg/mL dose gave responses that were slightly higher than the 0.1 mg/mL dose for some materials (metal/metal oxides) but not others (mostly carbon based ENM). For several carbon based ENM (carbon blacks, fullerenes, several CNTs), an inverse DCFH response is seen with increasing concentration (e.g. N110, F_soot, SWCNT_L). ENM with higher SSA tended to give a higher magnitude of decrease in the response (e.g. SWCNT_L vs. SWCNT_S vs. N110 with SSA of 510.5, 343, and 110 m^2/g , respectively).

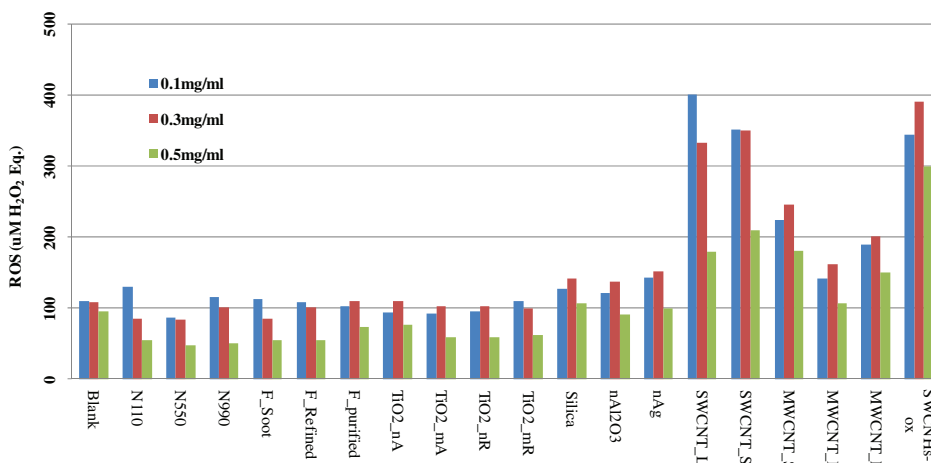


FIGURE 5. Dose response for the whole series of nanomaterials studied at three concentrations: 0.1, 0.3, and 0.5 mg/ml. The data are for Triton-X probe sonication, the condition with overall better dispersion efficiency and stability. Lack of a linear relationship with increased concentration is apparent. The lowest response was consistently observed for the highest concentrations. Depending on the nanomaterial type, especially for the carbon based nanomaterials, an inverse linear DCFH response is seen with increasing concentration (e.g. SWCNT_L and N110). The effect is higher for higher surface area nanomaterials. These anomalies are likely a net effect of several processes, such as potential absorption of DCFH reagent onto the surfaces of particles followed by removal from solution via agglomeration/precipitation and light scattering effects.

DISCUSSION

Nanomaterials have large surface area owing to higher particle number per unit mass than their micron-sized counterparts. This makes them highly reactive because surface atoms usually have unsatisfied high-energy bonds that will readily interact with other molecules to gain stability (Oberdorster *et al.* 2005; Doak *et al.* 2009). Enhanced adsorption onto ENM surface of the dyes or other chemical entities present in the reaction system, further modified by variable surface chemistries, manufacturing processes, and types of surfactants used to disperse ENM, may lead to measurement errors that are largely unknown (Belyanskaya *et al.* 2007; Doak *et al.* 2009). Few studies pointed to these limitations in the DTT assay (Sauvain *et al.* 2008) and DCFH assay (Doak *et al.* 2009); however, the evidence was mostly anecdotal. Several potentially serious analytical problems have been reported for the DCFH assay as early as 1999 (Rota *et al.* 1999a; Rota *et al.* 1999b; Myhre *et al.* 2003; Bonini *et al.* 2006) but they seem to have had little impact on adoption of the DCFH assay for ENM ROS measurements. Our finding that the DCFH assay is susceptible to several parameters and that the direction and magnitude of such effects varies unpredictably is in good agreement with these earlier cautionary reports.

Dispersion Efficiency

Proper dispersion of ENM for toxicological studies is a key factor and its significance has been recognized (Bihari *et al.* 2008). Yet, the problem has not been fully resolved and dispersions at the primary particle size continue to be challenging. In the present study, consistent with the best practices at the time, two types of dispersion mediums were tested, one biologically relevant medium of 1 % BSA/ 0.9 % NaCl_(aq) and the other, 0.07 % Triton-X 100, a nonionic surfactant routinely used for dispersing ENM. Agglomeration of ENM varies according to the sonication energy, frequency and time used and can impact ROS measurements (Murdock *et al.* 2008). Thus, both cup sonication (lower energy) and probe sonication (higher energy) were employed to disperse ENM in two media (1 % BSA / 0.9 % NaCl_{aq} and 0.07% Triton-X 100). The $d_{h,z,ave}$ and PDI results obtained (Table 2) indicate that, depending on the ENM class, dispersion efficiency can vary considerably. Dispersion stability and efficiency (with a few exceptions) was generally in the order: 1% BSA / 0.9% NaCl_{aq} with cup sonication < 1 % BSA / 0.9 % NaCl_{aq} with probe sonication < 0.07 % Triton X- 100 with probe sonication. In general, consistent with earlier reports (Allouni *et al.* 2009), carbon based ENM dispersed better than metal oxides under probe sonication and their agglomeration rates were slower than for metal oxides. This was reflected in the overall PDI values. Our dispersion efficiency (as reflected in the $d_{h,z,ave}$ and PDI values) were equivalent to or better than earlier results (Foucaud *et al.* 2007; Murdock *et al.* 2008; Bihari *et al.* 2008; Lu *et al.* 2009) performed with similar ENM.

While higher sonication energy can generally lead to better dispersions and smaller agglomerate size for some ENM, it can also lead to changes in ENM structure and even ENM breakage and generation of free radicals, which may induce biologically significant structural alterations in serum proteins (such as BSA) and other biological surfactants frequently used as dispersion media (Wang *et al.* 2009). For example, materials with high aspect ratios (SWCNT and MWCNT series) as well as those whose primary particle size is in the micron range (TiO₂-mA, TiO₂-mR and silica) had fluctuations in $d_{h,z,ave}$ and PDI. Moreover, the % intensity of the primary peak in the PSD fluctuated as well. Overall these factors point to a variable rate of agglomeration in dispersions of these materials. DLS data and SEM/TEM images of SWCNTs and micron-size TiO₂ confirmed structural fragmentations. This phenomenon was consistent with earlier observation of TiO₂ breakage (Mandzy *et al.* 2005). For the micron-size crystalline silica (with sizes typically in the 1-5 µm range), electron microscopy revealed a substantial fraction of smaller (<1 µm) particles. The $d_{h,z,ave}$ for crystalline silica may reflect a combination of these smaller particles and potential fragmentations. For TiO₂-Anatase particles, the dispersion was not as effective, consistent with the prior observations (Bihari *et al.* 2008).

It is speculated that the values for Al₂O₃ and the fullerene series (especially F_purified), are not representative of the true particle size distribution in the dispersions. They showed the highest rate of agglomeration of all the ENM studied, even though measurements were taken instantaneously after sonication. The PDI values obtained for these ENM were higher (approx 0.6-0.7) than the average PDI for the other ENM tested.

While these modifications may be less important relatively, for acellular than cellular assays, the use of high sonication energy may need to be balanced against these undesirable effects. Measuring particle size of CNTs by DLS might be error-prone (as stated in method section), but for our study it is sufficient for obtaining an idea of their hydrodynamic diameter in the dispersions. This is especially the case for their agglomeration rate in different mediums under different dispersion conditions. It was found that poorer dispersion leads to a larger average diameter ($d_{h,z,ave}$) for CNTs. Dispersion efficiency is likely a major contributor to the observed variability in ROS values (the 95% CI around the mean). This is easier noticed by looking at the 95% CI for the same material under different dispersion conditions (e.g. CNTs in 0.07 % Triton X-100 vs. 1% BSA / 0.9% NaCl_(aq)). However, it should be pointed out that dispersion is not a DCFH-specific problem.

ROS measurements

Different measurement times have been reported in the literature for the DCFH assay spanning from minutes to one hour (Foucaud *et al.* 2007; Veranth *et al.* 2007; Lu *et al.* 2009; Rothen-Rutishauser *et al.* 2010). Initially we investigated reaction kinetics for all tested ENM over 120 min (Figure 6). Under the current assay conditions, none of the reactions reached completion, and this may be in part due to continued auto-oxidation of the large DCFH pool. During the first 40 min, distinct reaction dynamics were observed for different ENM depending on dispersion media and sonication and the relative ranking of ENM ROS generation would change depending on the time of measurement. Meaningful measurements and comparisons among ENM leading to stable rankings of ENM ROS intrinsic potency could be made after 60 min. Reaction completion was observed at 90 min for higher reactant (DCFH and ENM) concentrations. We reported data for 90 min as a more conservative approach, although the results and conclusions of this work would not change if data were reported for 60 min. The reaction kinetics data have several implications. Because only a minor fraction of the reaction is completed in the first 10 min, DCFH measurements based on this time frame for individual ENM have little value. Even for comparative purposes, such as for relative ranking of their intrinsic potency to generate ROS, such measurements are unreliable if they are based on short time frames, especially < 40 min. Sixty minutes or more is necessary.

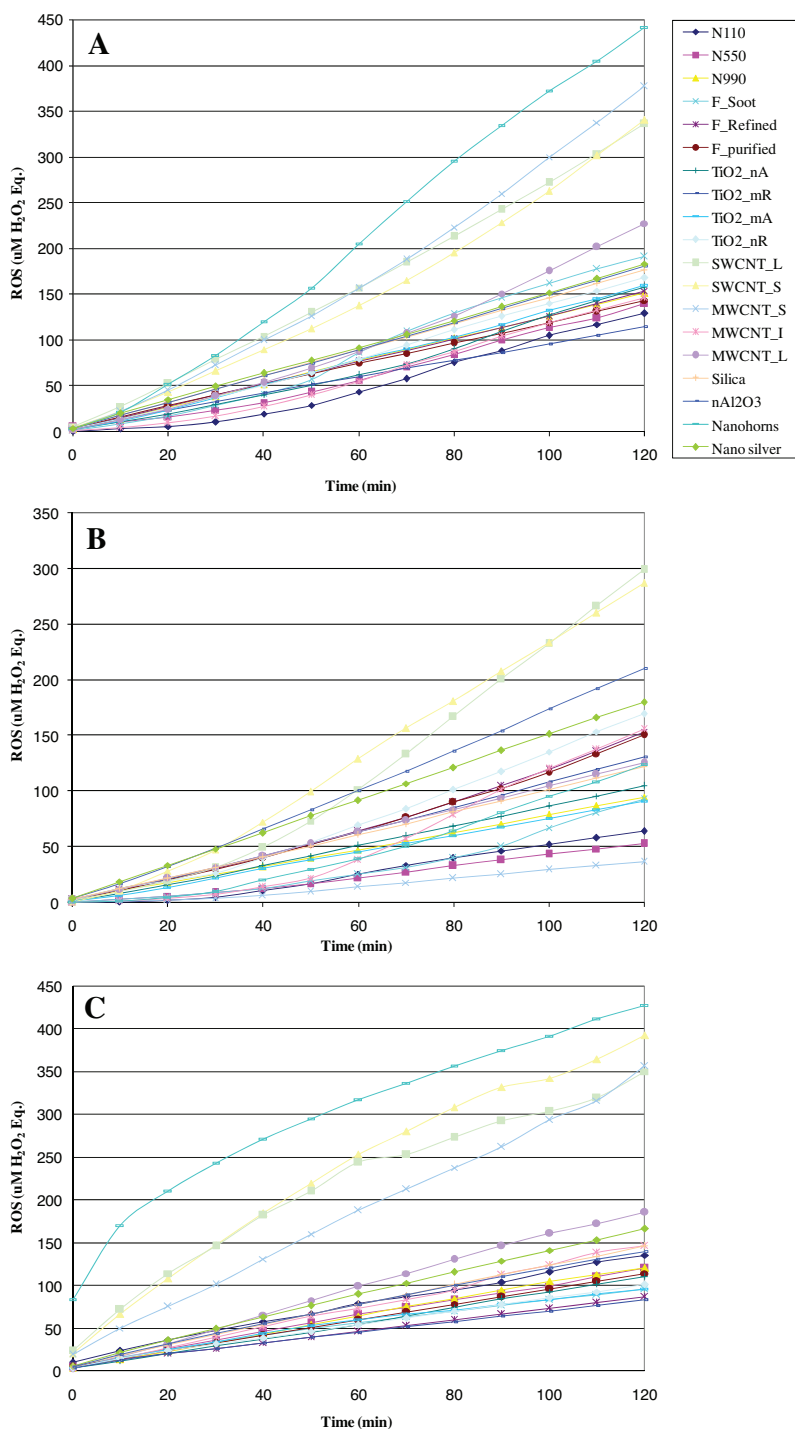


FIGURE 6. Reaction kinetics for the set of 19 ENM under various dispersion conditions for the 0.3 mg/mL concentration: (A) 1 wt.% BSA/0.9wt.% NaCl_(aq) and cup sonication; (B) 1% wt.BSA/0.9wt.% NaCl_(aq) and probe sonication; (C) 0.07% wt Triton-X and probe sonication.

Consistent with previous reports on DCFH oxidation by HRP, our results document significant effects of HRP on DCFH oxidation. More problematic is the finding that the magnitude of this effect varies depending on the dispersion media and sonication conditions, making corrections for such effects impossible. The range of H_2O_2 Eq. ROS generated as a result of DCFH oxidation by reactants other than ENM spanned from 100 (blank without HRP) to 800 $\mu\text{M H}_2\text{O}_{2(\text{eq})}$ (blank with HRP and probe sonication). The range of $\text{H}_2\text{O}_{2(\text{eq})}$ ROS generated as a result of DCFH oxidation by ENM without HRP was ~ 100 (blank) to $< 400 \mu\text{M H}_2\text{O}_{2(\text{eq})}$ under all conditions. These data do not support addition of HRP to ENM.

Another important factor, often overlooked, which may add to the variability of ROS measurements induced by ENM in the presence of HRP in the DCFH assay is the potential interaction and inactivation of HRP as a result of absorption onto ENM surfaces, as has been shown for silica nanoparticles and HRP, lysozyme, trypsin, and catalase (Vertegel *et al.* 2004). The magnitude of this effect, which may lead to different levels of HRP activity and DCFH oxidation, will likely depend on ENM type and particle size. Such concerns are contrary to a general tendency where HRP is being added during DCFH assay to ‘amplify the DCFH oxidation’ (Foucaud *et al.* 2007; Jiang *et al.* 2008; Rothen-Rutishauser *et al.* 2010). As mentioned previously, several M^{2+} transition metals (Co, Mn, Ni) common in CNTs and metal oxides may inactivate or enhance HRP catalytic activity with different potencies. For the reasons stated above, addition of HRP to ENM severely compromises the quality of the data, (which in the DCFH assay are inherently compromised by DCFH auto-oxidation) and renders comparisons inconsequential as one would not know how much effective ROS is generated by each ENM, given their variable physio-chemical characteristics and unknown re/activity to HRP.

In our tests, the DCFH gave consistently negative responses for the majority of ENM, irrespective of dispersion medium and method used. This is primarily driven by the high ROS values obtained for blanks (without ENM) and reflects one major inherent limitation of the assay: auto oxidation. This fact is consistent with other studies (Foucaud *et al.* 2007; Lu *et al.* 2009; Rothen-Rutishauser *et al.* 2010). Notable also is the fact that the majority of ENM that were negative gave values than were below the blank. For a reliable assay, a ROS value below blank would mean that the ENM exhibits antioxidant properties and the difference from blank value would be proportional to its intrinsic potency. This is unlikely to be the case for the majority of these ENM (with the exception perhaps of purified fullerenes). The more likely explanation for these observations is a net effect of several aforementioned ENM-induced artifacts that drive the overall DCFH response towards smaller values.

Only two ENM were positive under all three conditions (SWCNT_L, SWCNT_S). The number of positives varied with the dispersion medium

and sonication conditions between 3 and 5. A few CNTs switched from positive to negative and vice-versa upon dispersion/sonication conditions. Some typical cases involved nano silver (1/3 positive), MWCNT_S and _L (1/3 inconclusive) and SWCNH-ox. The SWCNH-ox represents an even more drastic example. For 2/3 conditions (1% BSA / 0.9% NaCl/ cup sonication and Triton X-100/probe sonication) SWCNH-ox gave one of the highest ROS values. However, in 1% BSA / 0.9% NaCl medium with probe sonication the result was conclusively negative. The reason for this drastic shift in behavior is not known and it warrants further investigations. For all the aforementioned reasons, negative DCFH results for ENM should be treated as uninformative. Additionally, reports of individual acellular DCFH results for ENM for which no blank values were provided or which have been acquired with the addition of HRP to ENM should be treated with skepticism.

Lack of a linear dose-response over the tested 0.1-0.5 mg/mL range is also concerning. For the series of carbon blacks, fullerenes, CNT and TiO₂ an inverse dose response was observed. For the remainder ENM (TiO₂ series, Silica, nAl₂O₃, nAg, MWCNTs and SWCNHs-ox) ROS values increased as concentration increased from 0.1 to 0.3 mg/mL but decreased for 0.5 mg/mL. This effect for the DCFH assay was also observed by Doak *et al.* 2009 for one type of ENM (iron oxides). Since only negligible fluorescence responses were obtained from ENM when they were run as blanks without DCFH (data omitted), factor associated with the reagent (DCFH) and its interaction with ENM must be responsible for such phenomena (non-linear response, high blank values, high variability in ROS measurements, many ENM resulting in responses below blank values, etc.). Although the mechanisms contributing to these observations have not been studied in detail and these effects have not been quantified, they can be attributed to several processes: adsorption of DCFH onto the surface of ENM (and the subsequent fluorescence quenching), ENM reagglomeration and sedimentation from solution, and light scattering or absorption by several ENM.

These findings are based on a cell-free system. The DCFH assay is also commonly used for quantitating the extracellular and intracellular oxidative stress in the presence of ENM. Since there are reasons to believe that problems with the acellular DCFH assay may also occur in the cellular DCFH assay, more rigorous method development and evaluation may be needed in order to quantify and minimize ROS measurement errors in cellular systems. The problems with the acellular DCFH assay for ENM ROS measurements raise concerns that similar problems may also happen in intracellular milieu. Since the medium complexity is greater, the variability and uncertainty in DCFH measurements in cellular systems may be even greater. As for the intracellular DCFH measurements, one important factor is the ENM type and the extent of its intracellular

uptake. In the best case scenario, there is always the auto oxidation of DCFH by visible light to worry about (Marchesi *et al.* 1999).

CONCLUSIONS

The acellular DCFH assay for measuring ROS elicited by ENM is susceptible to experimental conditions and the assay lacks robustness and reproducibility required in an analytical method. Its broad adoption for ENM ROS measurements without sufficient method development and validation may lead to erroneous and conflicting data. Although further modifications and development may improve its performance, the inherent limitations of the assay are a serious obstacle. We advocate for the discontinuation of the DCFH assay for measuring ROS elicited by ENM and encourage exploration of alternative more biologically relevant assays.

ACKNOWLEDGEMENTS/DISCLAIMERS

One of the authors (AKP) would like to dedicate this work to his dear friend, Mr. Yogesh Rawat, whose life was cut short by a tragic accident. Yogesh' enthusiasm for life and studies was contagious and has had a strong influence in shaping his academic ambitions.

We would like to thank Mr. Neeraj Pardhy, from Dept. of Plastics Engineering, Prof. Jackie Zhang from Dept. of Civil and Environmental Engineering, Mr. Srikanth Ammu and Prof. Sanjeev Manohar from Dept of Chemical Engineering and Mr. Abhishek Kumar from Dept. of Physics for their assistance with some aspects of the experimental work. This study was supported through the Nanoscale Science and Engineering Centers Program of the National Science Foundation # 0425826.

ABBREVIATIONS

ENM: Engineered Nanomaterial(s),
one or more dimensions < 100 nm
ROS: Reactive oxygen species
RNS: Reactive nitrogen species
DCFH/DCF: Dichlorofluorescein
CNTs: Carbon nanotubes
BOD: Biological oxidative damage
EPR: Electron paramagnetic resonance
ESR: Electron spin resonance
OS: Oxidative stress
DTT: Dithiothreitol
HRP: Horseradish peroxidase
DLS: Dynamic light scattering
 $d_{h,z,ave}$: Z-average hydrodynamic diameter
PDI: Particle size polydispersity index

REFERENCES

- Alloumi ZE, Cimpan MR, Hol PJ, Skodvin T, Gjerdet NR. 2009. Agglomeration and sedimentation of TiO₂ nanoparticles in cell culture medium. *Colloids Surf B Biointerfaces* 68(1): 83-87
- Arbab AS, Bashaw LA, Miller BR, Jordan EK, Lewis BK, Kalish H, Frank JA. 2003. Characterization of biophysical and metabolic properties of cells labeled with superparamagnetic iron oxide nanoparticles and transfection agent for cellular MR imaging. *Radiology* 229(3): 838-846
- Ayres JG, Borm P, Cassee FR, Castranova V, Donaldson K, Ghio A, Harrison RM, Hider R, Kelly F, Kooter IM, Marano F, Maynard RL, Mudway I, Nel A, Sioutas C, Smith S, Baeza-Squiban A, Cho A, Duggan S, Froines J. 2008. Evaluating the Toxicity of Airborne Particulate Matter and Nanoparticles by Measuring Oxidative Stress Potential - A Workshop Report and Consensus Statement. *Inhalation Toxicology* 20(1): 75-99
- Bekyarova GY, Ivanova DG, Madjova VH. 2007. Molecular mechanisms associating oxidative stress with endothelial dysfunction in the development of various vascular complications in diabetes mellitus. *Folia Med (Plovdiv)* 49(3-4): 13-19
- Bello D, Hsieh S-F, Schmidt D, Rogers E. 2009. Nanomaterials properties vs. biological oxidative damage: Implications for toxicity screening and exposure assessment. *Nanotoxicology* 3(3): 249 – 261
- Belyanskaya L, Manser P, Spohn P, Bruinink A, Wick P. 2007. The reliability and limits of the MTT reduction assay for carbon nanotubes-cell interaction. *Carbon* 45(13): 2643-2648
- Bihari P, Vippola M, Schultes S, Praetner M, Khandoga AG, Reichel CA, Coester C, Tuomi T, Rehberg M, Krombach F. 2008. Optimized dispersion of nanoparticles for biological in vitro and in vivo studies. *Particle and Fibre Toxicology* 5: 14
- Bonini MG, Rota C, Tomasi A, Mason RP. 2006. The oxidation of 2',7'-dichlorofluorescein to reactive oxygen species: a self-fulfilling prophesy? *Free Radic Biol Med* 40(6): 968-975
- Bonomini F, Tengattini S, Fabiano A, Bianchi R, Rezzani R. 2008. Atherosclerosis and oxidative stress. *Histol Histopathol* 23(3): 381-390
- Borm PJA, Kelly F, Káňal/Anzli N, Schins RPF, Donaldson K. 2007. Oxidant generation by particulate matter: from biologically effective dose to a promising, novel metric. *Occupational and Environmental Medicine* 64(2): 73-74
- Calabrese V, Guagliano E, Sapienza M, Mancuso C, Butterfield DA, Stella AM. 2006. Redox regulation of cellular stress response in neurodegenerative disorders. *Ital J Biochem* 55(3-4): 263-282
- Casey A, Davoren M, Herzog E, Lyng FM, Byrne HJ, Chambers G. 2007. Probing the interaction of single walled carbon nanotubes within cell culture medium as a precursor to toxicity testing. *Carbon* 45(1): 34-40
- Chen X, Zhong Z, Xu Z, Chen L, Wang Y. 2010. 2,7-Dichlorodihydrofluorescein as a fluorescent probe for reactive oxygen species measurement: Forty years of application and controversy. *Free Radical Research* 44: 587-604
- Degli-Esposti M, Pon LA, Schon EA. 2001. Chapter 4 Assessing functional integrity of mitochondria in vitro and in vivo. In: *Methods in Cell Biology*: Academic Press, 75-96
- Doak SH, Griffiths SM, Manshian B, Singh N, Williams PM, Brown AP, Jenkins GJ. 2009. Confounding experimental considerations in nanogenotoxicology. *Mutagenesis* 24(4): 285-293
- Donaldson K, Poland CA, Schins RPF. 2010. Possible genotoxic mechanisms of nanoparticles: Criteria for improved test strategies. *Nanotoxicology* early print: 1-7
- Forbes JM, Coughlan MT, Cooper ME. 2008. Oxidative stress as a major culprit in kidney disease in diabetes. *Diabetes* 57(6): 1446-1454
- Foucaud L, Wilson MR, Brown DM, Stone V. 2007. Measurement of reactive species production by nanoparticles prepared in biologically relevant media. *Toxicology Letters* 174(1-3): 1-9
- Hilding J, Grulke EA, Zhang ZG, Lockwood F. 2003. Dispersion of Carbon Nanotubes in Liquids. *Journal of Dispersion Science and Technology* 24(1): 1 – 41
- Hsiai T, Berliner JA. 2007. Oxidative stress as a regulator of murine atherosclerosis. *Curr Drug Targets* 8(12): 1222-1229
- Hurt RH, Monthieux M, Kane A. 2006. Toxicology of carbon nanomaterials: Status, trends, and perspectives on the special issue. *Carbon* 44(6): 1028-1033.
- Jiang J, Oberdorster G, Elder A, Gelein R, Mercer P, Biswas P. 2008. Does nanoparticle activity depend upon size and crystal phase? *Nanotoxicology* 2(1): 33-42
- Kato T, Hiraga Y, Takahashi Y, Kinoshita T. 1979. Determination of serum uric acid and glucose using dichlorofluorescein-cycloheptaamylose complex. *Chem Pharm Bull (Tokyo)* 27(12): 3073-3077

- Krause, B., Mende, M., Po^ottschke P., Petzold G., 2010. Dispersability and particle size distribution of CNTs in an aqueous surfactant dispersion as a function of ultrasonic treatment time. *Carbon*, 48, 2746–2754.
- Lau AT, Wang Y, Chiu JF. 2008. Reactive oxygen species: current knowledge and applications in cancer research and therapeutic. *J Cell Biochem* 104(2): 657-667
- Lu S, Duffin R, Poland C, Daly P, Murphy F, Drost E, Macnee W, Stone V, Donaldson K. 2009. Efficacy of simple short-term in vitro assays for predicting the potential of metal oxide nanoparticles to cause pulmonary inflammation. *Environ Health Perspect* 117(2): 241-247
- Maynard AD. 2006. *Nanotechnology: A Research Strategy for Addressing Risk* Washington DC, Woodrow Wilson International Center for Scholars.
- Mahmoudi A, Nazari K, Mohammadian N, Moosavi-Movahedi A. 2003. Effect of Mn²⁺, Co²⁺, Ni²⁺, and Cu²⁺ on horseradish peroxidase. Activation, inhibition, and denaturation studies. *Applied Biochemistry and Biotechnology* 104(1): 81-94
- Mandzy N, Grulke E, Druffel T. 2005. Breakage of TiO₂ agglomerates in electrostatically stabilized aqueous dispersions. *Powder Technology* 160(2): 121-126
- Manna SK, Sarkar S, Barr J, Wise K, Barrera EV, Jejelowo O, Rice-Ficht AC, Ramesh GT. 2005. Single-walled carbon nanotube induces oxidative stress and activates nuclear transcription factor-kappaB in human keratinocytes. *Nano Lett* 5(9): 1676-1684
- Marchesi E, Rota C, Fann YC, Chignell CF, Mason RP. 1999. Photoreduction of the fluorescent dye 2'-7'-dichlorofluorescein: a spin trapping and direct electron spin resonance study with implications for oxidative stress measurements. *Free Radic Biol Med* 26(1-2): 148-161
- Mates JM, Segura JA, Alonso FJ, Marquez J. 2008. Intracellular redox status and oxidative stress: implications for cell proliferation, apoptosis, and carcinogenesis. *Arch Toxicol* 82(5): 273-299
- Meng H, Xia T, George S, Nel AE. 2009. A Predictive Toxicological Paradigm for the Safety Assessment of Nanomaterials. *ACS Nano* 3(7): 1620-1627
- Monteiro-Riviere NA, Inman AO. 2006. Challenges for assessing carbon nanomaterial toxicity to the skin. *Carbon* 44(6): 1070-1078
- Monteiro-Riviere NA, Inman AO, Zhang LW. 2009. Limitations and relative utility of screening assays to assess engineered nanoparticle toxicity in a human cell line. *Toxicol Appl Pharmacol* 234(2): 222-235
- Moore VC, Strano MS, Haroz EH, Hauge RH, Smalley RE, Schmidt J, Talmon Y. 2003. Individually Suspended Single-Walled Carbon Nanotubes in Various Surfactants. *Nano Letters* 3(10): 1379-1382
- Murdock RC, Braydich-Stolle L, Schrand AM, Schlager JJ, Hussain SM. 2008. Characterization of Nanomaterial Dispersion in Solution Prior to In Vitro Exposure Using Dynamic Light Scattering Technique. *Toxicol Sci* 101(2): 239-253
- Myhre O, Andersen JM, Aarnes H, Fonnum F. 2003. Evaluation of the probes 2',7'-dichlorofluorescein diacetate, luminol, and lucigenin as indicators of reactive species formation. *Biochemical Pharmacology* 65(10): 1575-1582
- Nastassja L, Vicki C, Rebekah D. 2008. Cytotoxicity of Nanoparticles. *Small* 4(1): 26-49.
- Nel A, Xia T, Madler L, Li N. 2006. Toxic Potential of Materials at the Nanolevel. *Science* 311(5761): 622-627
- Nishikawa M. 2008. Reactive oxygen species in tumor metastasis. *Cancer Lett* 266(1): 53-59
- Oberdorster G, Oberdorster E, Oberdorster J. 2005. Nanotoxicology: an emerging discipline evolving from studies of ultrafine particles. *Environ Health Perspect* 113(7): 823-839
- Paravicini TM, Touyz RM. 2008. NADPH oxidases, reactive oxygen species, and hypertension: clinical implications and therapeutic possibilities. *Diabetes Care* 31 Suppl 2: S170-180.
- Raimondi F, Scherer GG, Kotz R, Wokaun A. 2005. Nanoparticles in energy technology: Examples from electrochemistry and catalysis. *Angew Chem Int Ed* 44(15):2190–2209.
- Rogers EJ, Bello D, Hsieh S-F. 2008. Oxidative Stress as a Screening Metric of Potential Toxicity by Nanoparticles and Airborne Particulate Matter. *Inhalation Toxicology* 20(9): 895
- Rota C, Chignell CF, Mason RP. 1999a. Evidence for free radical formation during the oxidation of 2'-7'-dichlorofluorescein to the fluorescent dye 2'-7'-dichlorofluorescein by horseradish peroxidase: possible implications for oxidative stress measurements. *Free Radic Biol Med* 27(7-8): 873-881
- Rota C, Fann YC, Mason RP. 1999b. Phenoxyl Free Radical Formation during the Oxidation of the Fluorescent Dye Dichlorofluorescein by Horseradish Peroxidase. *Journal of Biological Chemistry* 274(40): 28161-28168

- Rothen-Rutishauser B, Brown DM, Piallier-Boyles M, Kinloch IA, Windle AH, Gehr P, Stone V. 2010. Relating the physicochemical characteristics and dispersion of multiwalled carbon nanotubes in different suspension media to their oxidative reactivity in vitro and inflammation in vivo. *Nanotoxicology* 4(3): 331-342
- Salata O. 2004. Applications of nanoparticles in biology and medicine. *J Nanobiotechnol* 2(1):1-6.
- Saran N, Parikh K, Suh D-S, Munoz E, Kolla H, Manohar SK. 2004. Fabrication and Characterization of Thin Films of Single-Walled Carbon Nanotube Bundles on Flexible Plastic Substrates. *Journal of the American Chemical Society* 126(14): 4462-4463
- Sarvazyan N. 1996. Visualization of doxorubicin-induced oxidative stress in isolated cardiac myocytes. *Am J Physiol* 271(5 Pt 2): H2079-2085
- Sauvain J-J, Deslarzes S, Riediker M. 2008. Nanoparticle reactivity toward dithiothreitol. *Nanotoxicology* 2(3): 121 – 129
- Suzuki O, Oya M, Katsumata Y, Matsumoto T, Yada S. 1980. A new enzymatic method for the demonstration of spermine in human seminal stains. *J Forensic Sci* 25(1): 99-102
- Tarpey MM, Fridovich I. 2001. Methods of Detection of Vascular Reactive Species: Nitric Oxide, Superoxide, Hydrogen Peroxide, and Peroxynitrite. *Circ Res* 89(3): 224-236
- Valko M, Morris H, Cronin MT. 2005. Metals, toxicity and oxidative stress. *Curr Med Chem* 12(10): 1161-1208
- Valko M, Rhodes CJ, Moncol J, Izakovic M, Mazur M. 2006. Free radicals, metals and antioxidants in oxidative stress-induced cancer. *Chem Biol Interact* 160(1): 1-40
- Veranth JM, Kaser EG, Veranth MM, Koch M, Yost GS. 2007. Cytokine responses of human lung cells (BEAS-2B) treated with micron-sized and nanoparticles of metal oxides compared to soil dusts. *Part Fibre Toxicol* 4: 2
- Vertegel AA, Siegel RW, Dordick JS. 2004. Silica nanoparticle size influences the structure and enzymatic activity of adsorbed lysozyme. *Langmuir* 20(16): 6800-6807
- Wang H, Joseph JA. 1999. Quantifying cellular oxidative stress by dichlorofluorescein assay using microplate reader. *Free Radic Biol Med* 27(5-6): 612-616
- Wang J, Wang YF, Gao J, Hu P, Guan HY, Zhang LQ, et al. 2009. Investigation on damage of BSA molecules under irradiation of low frequency ultrasound in the presence of Fe-III-tartrate complexes. *Ultrason Sonochem* 16(1):41-49.
- Wilson MR, Lightbody JH, Donaldson K, Sales J, Stone V. 2002. Interactions between ultrafine particles and transition metals in vivo and in vitro. *Toxicol Appl Pharmacol* 184(3): 172-179
- Wörle-Knirsch JM, Pulskamp K, Krug HF. 2006. Oops They Did It Again! Carbon Nanotubes Hoax Scientists in Viability Assays. *Nano Letters* 6(6): 1261-1268
- Xia T, Kovochich M, Brant J, Hotze M, Sempf J, Oberley T, Sioutas C, Yeh JI, Wiesner MR, Nel AE. 2006. Comparison of the abilities of ambient and manufactured nanoparticles to induce cellular toxicity according to an oxidative stress paradigm. *Nano Lett* 6(8): 1794-1807
- Xia T, Li N, Nel AE. 2009. Potential Health Impact of Nanoparticles. *Annual Review of Public Health* 30(1): 137-150
- Zhang WX. 2003. Nanoscale iron particles for environmental remediation: An overview. *J Nanopart Res* 5(3-4):323-332.